

Production of relativistic positronium in collisions of photons and electrons with nuclei and atoms

S. R. Gevorkyan and E. A. Kuraev

Laboratory of Theoretical Physics, Joint Institute for Nuclear Research, Dubna 141980, Russia

A. Schiller

Institut für Theoretische Physik and Naturwissenschaftlich-Theoretisches Zentrum, Universität Leipzig, D-04109 Leipzig, Germany

V. G. Serbo

Department of Physics, Novosibirsk State University, Novosibirsk 630090, Russia

A. V. Tarasov

Laboratory of Theoretical Physics, Joint Institute for Nuclear Research, Dubna 141980, Russia

(Received 10 April 1998)

We consider the production of ultrarelativistic positronium (Ps) in $\gamma A \rightarrow \text{Ps} + A$ and $eA \rightarrow \text{Ps} + eA$ processes, where A is an atom or a nucleus with charge Ze . For the photoproduction of para- and ortho-Ps and the electroproduction of para-Ps we obtain the most complete description compared to previous works. It includes high-order $Z\alpha$ corrections and polarization effects. The accuracy of the obtained cross sections is determined by omitted terms of the order of the inverse Ps Lorentz factor. The high-order multi-photon electroproduction of ortho-Ps studied dominates for the collision of electrons with heavy atoms over the bremsstrahlung production from the electron via a virtual photon proposed by Holvik and Olsen [Phys. Rev. D **35**, 2124 (1987)]. Our results complete and correct the studies of those authors. [S1050-2947(98)03112-6]

PACS number(s): 36.10.Dr, 13.60.-r, 13.85.Qk, 12.20.-m

I. INTRODUCTION

The production of relativistic positronium (Ps) opens an attractive possibility to create intensive beams of elementary atoms. It is known that e^+e^- elementary atoms exist in two spin states: parapositronium (para-Ps, singlet state) 1S_0 with lifetime at rest $\tau_0 = 0.123$ ns and orthopositronium (ortho-Ps, triplet state) 3S_1 with $\tau_0 = 0.14$ μ s. The relativistic Ps with lifetime $\tau = \gamma_{\text{Ps}}\tau_0$ (where γ_{Ps} is its Lorentz factor) can be detected far from its creation point, which is quite useful from the experimental point of view.

The main motivations to study the positronium production can be summarized as follows. (i) It is the simplest hydrogenlike atom that is very convenient for testing fundamental properties of nature such as the *CPT* theorem (see Ref. [1]). (ii) There is an essential difference between experimental measurements and theoretical calculations of the ortho-Ps width [2]. (iii) Finally, the relativistic Ps has an unusual large transparency in thin layers (see Ref. [3] and references therein); in QCD a similar property is called color transparency.

In this paper we consider the Ps production in the collision of high-energy photons and electrons with nuclei or atoms A of charge Ze (Figs. 1 and 2):

$$\gamma A \rightarrow \text{Ps} + A, \quad eA \rightarrow \text{Ps} + eA. \quad (1.1)$$

Due to charge parity conservation, the number of photons exchanged between the projectile photon and the target nucleus has to be odd or even for the production of para-Ps or ortho-Ps, respectively.

Let us briefly summarize the present status of calculating the photo- and electroproduction of relativistic positronium. The photoproduction of para-Ps was calculated in the main logarithmic approximation in [4] and more precisely in [5]. In both papers the effects of high-order corrections in the parameter ν ,

$$\nu = Z\alpha = Z \frac{e^2}{4\pi} \approx Z/137, \quad (1.2)$$

were not taken into account. In Eq. (1.2) Ze denotes the nucleus charge. However, the parameter ν is of the order of 1 for heavy nuclei and therefore the whole series in ν has to be summed. These ν effects were considered for para- and ortho-Ps photoproduction in [6], but only for total cross sections with complete screening. Polarization effects of the photon projectile and azimuthal asymmetries in the Ps distribution have not been studied. The electroproduction of para-Ps was calculated in [4,7,8] without high-order ν cor-

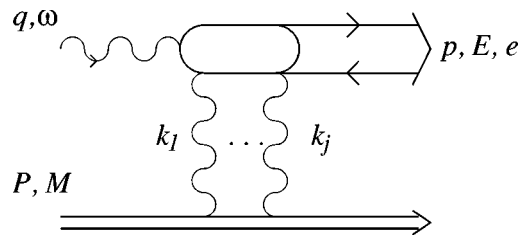


FIG. 1. Photoproduction of Ps on the nucleus with an odd (even) number j of exchanged photons for para-Ps (ortho-Ps).

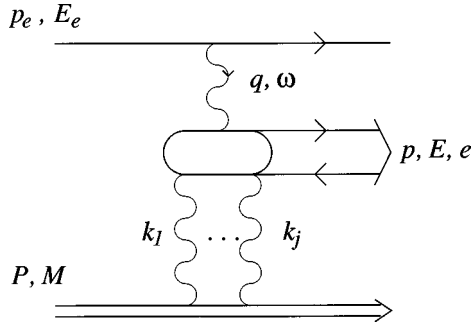


FIG. 2. Electroproduction of Ps on the nucleus.

reactions. The corresponding ortho-Ps was considered in [7,8], where only the bremsstrahlung production of Fig. 3 was examined.

The outline of our paper is as follows. In Sec. II we obtain the most complete description of the para- and ortho-Ps photoproduction on nuclei and atoms taking into account polarization, high-order corrections in ν , and screening effects of target atoms. First the general matrix elements for the Ps production in virtual photon nucleus scattering is presented. Differential and total cross sections for para- and ortho-Ps photoproduction are calculated in the following subsections. Section III is devoted to the electroproduction of relativistic positronium. Our exact results for the para-Ps production are compared with calculations using the equivalent photon approximation and neglecting high-order ν contributions. In Sec. III C we present an additional mechanism for electroproduction of ortho-Ps, namely, the multiphoton production (summed over two, four, six, etc. exchanged photons) of Fig. 2. We show that it may be more important than the bremsstrahlung mechanism of Fig. 3 and even dominates for heavy atoms. In Sec. IV we summarize our results.

Our main notations are given in Figs. 1 and 2: a photon with four-momentum q and energy ω or an electron with four-momentum p_e and energy E_e collides with a nucleus of four-momentum P , mass M and charge Ze and produces Ps described by four-momentum p , energy E and polarization four-vector e . We denote by m_e the electron mass. The mass of the e^+e^- bound state and a convenient abbreviation are

$$m_{\text{Ps}} \approx 2m_e, \quad \sigma_0 = \pi \nu^2 \frac{\alpha^4}{m_e^2}. \quad (1.3)$$

In the electroproduction of Ps (Fig. 2) we deal with a virtual photon generated by the electron. For this photon we use the notation

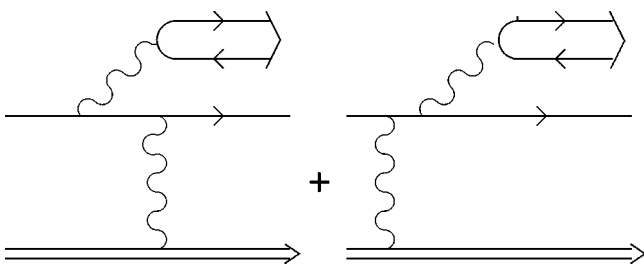


FIG. 3. Bremsstrahlung production of ortho-Ps on the nucleus.

$$Q^2 = -q^2 > 0, \quad y = \frac{Q^2}{4m_e^2}, \quad \mu = m_e \sqrt{1+y}. \quad (1.4)$$

Throughout the paper we consider the production of relativistic Ps, which means that we consider the energy region

$$\begin{aligned} \omega \approx E \gg 2m_e & \text{ for } \gamma A \rightarrow \text{Ps} + A, \\ E_e > \omega \approx E \gg 2m_e & \text{ for } eA \rightarrow \text{Ps} + eA. \end{aligned} \quad (1.5)$$

II. PHOTOPRODUCTION OF POSITRONIUM

A. General matrix element for the reaction $\gamma^*A \rightarrow \text{Ps} + A$

In this subsection we assume that the photon q is virtual, $q^2 = -Q^2 < 0$, and obtain formulas that will be useful for both photo- and electroproduction of Ps. Choosing the z axis along the photon momentum, the polarization vector for the transverse photon (T photon γ_T^* with helicity $\lambda_\gamma = \pm 1$) is

$$e_\gamma = (0, e_{\gamma x}, e_{\gamma y}, 0).$$

Taking into account gauge invariance, the polarization vector for the scalar photon (S photon γ_S^* with helicity $\lambda_\gamma = 0$) can be chosen in the form

$$e_S = \frac{2\sqrt{Q^2}}{s} p_2, \quad p_2 = P - \frac{M^2}{s} q, \quad s = 2qP = 2\omega M.$$

In what follows we calculate all distributions to an accuracy neglecting only pieces of the order of

$$\frac{2m_e}{\omega}, \quad \frac{|\mathbf{p}_\perp|}{\omega}, \quad \frac{\sqrt{Q^2}}{\omega}. \quad (2.1)$$

Here \mathbf{p}_\perp is the transverse component of the Ps three-momentum. To this accuracy the momentum transfer squared to the nucleus is given by

$$t = (p - q)^2 = -4\mu^2(\tau + \epsilon^2), \quad \tau = \frac{\mathbf{p}_\perp^2}{4\mu^2}, \quad \epsilon = \frac{\mu}{\omega}. \quad (2.2)$$

The amplitudes of the $\gamma^*A \rightarrow \text{Ps} + A$ process are obviously closely related to those of the e^+e^- pair production in the field of a heavy nucleus (for equal electron and positron momenta $(\mathbf{p}_+ = \mathbf{p}_- = \mathbf{p}/2)$). For the latter amplitudes we use the convenient form that was recently obtained in [9]¹

¹Compare Eqs. (29), (30) and (40), (41) of [9], taking into account the equal momenta for e^\pm . Note that in the paper of Ivanov and Melnikov an unusual notation for $\hat{\mathbf{a}}$ has been used, which we would like to mention here: $\hat{\mathbf{a}} = \hat{a}$, where $\hat{a} = a_\mu \gamma^\mu$. In [9] it was also noticed that for the lepton pair production by a real incident photon, their expression for the amplitude (29) coincides with the known result in the literature [10,11].

$$\begin{aligned}
M(\gamma_T^* A \rightarrow e^+ e^- A) &= -\frac{Z(4\pi\alpha)^{3/2}}{\mu^3} \bar{u} \hat{p}_2 \left[(\mathbf{n} \mathbf{e}_\gamma + \hat{n} \hat{e}_\gamma) \Phi_s + i\nu \frac{2m_e}{\mu} \hat{e}_\gamma \Phi_t \right] v, \\
(2.3)
\end{aligned}$$

$$\begin{aligned}
M(\gamma_S^* A \rightarrow e^+ e^- A) &= \frac{Z(4\pi\alpha)^{3/2}}{\mu^3} i\nu \sqrt{\frac{Q^2}{\mu}} \Phi_t \bar{u} \hat{p}_2 v. \\
(2.4)
\end{aligned}$$

Here u and v are the spinors of the produced pair of electron and positron. Furthermore, the four-unit vector n is defined as

$$n = (0, \mathbf{n}, 0), \quad \mathbf{n} = \frac{\mathbf{p}_\perp}{|\mathbf{p}_\perp|}.$$

The functions Φ_s and Φ_t are given with the help of the Gauss hypergeometric function $F(a, b; c; z)$,

$$\begin{aligned}
\Phi_s \equiv \Phi_s(\tau, \nu, \epsilon) &= \frac{\sqrt{\tau}}{(\tau + \epsilon^2)(1 + \tau)} F(i\nu, -i\nu; 1; z) \frac{\pi\nu}{\sinh \pi\nu}, \\
(2.5)
\end{aligned}$$

$$\begin{aligned}
\Phi_t \equiv \Phi_t(\tau, \nu) &= \frac{1 - \tau}{(1 + \tau)^3} F(1 + i\nu, 1 - i\nu; 2; z) \frac{\pi\nu}{\sinh \pi\nu}, \\
(2.6)
\end{aligned}$$

$$z = \left(\frac{1 - \tau}{1 + \tau} \right)^2. \quad (2.7)$$

Let us briefly mention some main properties of these functions:

$$\Phi_s \rightarrow \frac{\sqrt{\tau}}{(\tau + \epsilon^2)(1 + \tau)}, \quad \Phi_t \rightarrow \frac{1}{1 - \tau^2} \ln \frac{(1 + \tau)^2}{4\tau} \quad \text{at } \nu \rightarrow 0;$$

$$\Phi_s \rightarrow \frac{\sqrt{\tau}}{(\tau + \epsilon^2)}, \quad \Phi_t \rightarrow \ln \frac{1}{4\tau} - 2f(\nu) \quad \text{at } \tau \rightarrow 0; \quad (2.8)$$

$$\Phi_s \rightarrow \frac{1}{2} \frac{\pi\nu}{\sinh \pi\nu}, \quad \Phi_t \rightarrow \frac{1}{8} (1 - \tau) \frac{\pi\nu}{\sinh \pi\nu} \quad \text{at } \tau \rightarrow 1;$$

$$\Phi_s \rightarrow \frac{1}{\tau^{3/2}}, \quad \Phi_t \rightarrow -\frac{1}{\tau^2} \left[\ln \frac{\tau}{4} - 2f(\nu) \right] \quad \text{at } \tau \rightarrow \infty.$$

The function $f(\nu)$ is well known [see Eq. (95,19) in [11]],

$$f(\nu) = \nu^2 \sum_{n=1}^{\infty} \frac{1}{n(n^2 + \nu^2)}. \quad (2.9)$$

For small ν values it behaves as $f(\nu) \approx \zeta(3) \nu^2$ with the Riemann zeta function

$$\zeta(3) = \sum_{n=1}^{\infty} \frac{1}{n^3} = 1.2021. \quad (2.10)$$

As the next step the spinors of the electron and positron are substituted by the wave function of positronium in quantum state n at the origin $\psi(0) = (m_e \alpha)^{3/2} / \sqrt{8\pi n^3}$ according to the rule (see, for example, [12]):

$$\bar{u}, \dots, v \rightarrow \frac{m_e \alpha^{3/2}}{\sqrt{4\pi n^3}} \frac{1}{4} \text{Tr}[\dots (\hat{p} + m_{\text{Ps}}) \Gamma]. \quad (2.11)$$

Here Γ is a projection operator to be chosen as $\Gamma = i\gamma^5$ for the para-Ps and $\Gamma = \hat{e}^*$ for the ortho-Ps state.

Now the amplitudes of Ps production by T or S photons can be obtained using Eqs. (2.3), (2.4), and (2.11). The para-Ps is produced only by transverse photons

$$M(\gamma_T^* A \rightarrow n^1 S_0 + A) = \frac{2\pi Z \alpha^3}{n^{3/2}} \frac{s}{m_e^2 (1+y)^{3/2}} (\mathbf{e}_\gamma \times \mathbf{n}) \cdot \frac{\mathbf{q}}{\omega} \Phi_s, \quad (2.12)$$

$$M(\gamma_S^* A \rightarrow n^1 S_0 + A) = 0. \quad (2.13)$$

For the ortho-Ps production there are two possibilities: The transversely polarized ortho-Ps (with helicity $\lambda = \pm 1$) arises from transverse photons only

$$M(\gamma_T^* A \rightarrow n^3 S_1 + A) = -i \frac{4\pi Z^2 \alpha^4}{n^{3/2}} \frac{s}{m_e^2 (1+y)^2} (\mathbf{e}_\gamma \cdot \mathbf{e}^*) \Phi_t, \quad (2.14)$$

while the longitudinally polarized ortho-Ps (with helicity $\lambda = 0$) is produced by scalar photons

$$M(\gamma_S^* A \rightarrow n^3 S_1 + A) = i \frac{\sqrt{Q^2} 4\pi Z^2 \alpha^4}{2m_e n^{3/2}} \frac{s}{m_e^2 (1+y)^2} \Phi_t. \quad (2.15)$$

From Eqs. (2.14) and (2.15) we observe that helicity is conserved in the $\gamma \rightarrow$ ortho-Ps transition, i.e., $\lambda_\gamma = \lambda$. We also notice that both amplitudes (2.14) and (2.15) do not depend on the azimuthal angle of ortho-Ps.

In the following subsections we study the production of positronium by real photons. Therefore, in all expressions we choose [see Eq. (1.4)] $Q^2 = 0$ and $y = 0$.

B. Photoproduction of para-Ps

The differential cross section of para-Ps production on nuclei can be obtained using the amplitude (2.12) at $Q^2 = 0$,

$$d\sigma_{\text{singlet}} = \frac{\sigma_0}{n^3} |\mathbf{e}_\gamma \times \mathbf{n}|^2 \Phi_s^2 d\tau \frac{d\varphi}{2\pi}, \quad (2.16)$$

where φ is the azimuthal angle of Ps. To describe the polarization degree of the initial photon in general, it is convenient to use Stokes parameters $\xi_{1,2,3}$. In that case Eq. (2.16) transforms to

$$d\sigma_{\text{singlet}} = \frac{\sigma_0}{2n^3} [1 + \xi_1 \sin 2\varphi - \xi_3 \cos 2\varphi] \Phi_s^2 d\tau \frac{d\varphi}{2\pi}. \quad (2.17)$$

We see that this cross section does not depend on ξ_2 , i.e., on the circular polarization of photon. Furthermore, the scattering plane is mainly orthogonal to the direction of the linear polarization of the photon. For $\xi_i \rightarrow 0$ and $\nu \rightarrow 0$ the result (2.17) coincides with that obtained in [5].

The dependence of cross section (2.17) on the Ps polar angle θ is completely described by the function $\Phi_s^2(\tau, \nu, \epsilon)$ since in our case

$$\tau = \left(\frac{\omega \theta}{2m_e} \right)^2. \quad (2.18)$$

According to Eq. (2.8), the function $\Phi_s(\tau, \nu, \epsilon)$ depends on ν only in the region $\tau \sim 1$, whereas for $\tau \ll 1$ and $\tau \gg 1$ the angular behavior of cross section (2.17) has a universal (independent of ν) character. In particular, in the region of very small angles

$$\frac{m_e^2}{\omega^2} \ll \theta \ll \frac{m_e}{\omega} \quad (2.19)$$

the differential cross section has a very simple form

$$d\sigma_{\text{singlet}} = \frac{\sigma_0}{n^3} \frac{d\theta}{\theta}.$$

The total cross section is obtained from Eq. (2.17) by integrating over φ and τ and by summing over all n^1S_0 quantum states:

$$\sigma_{\text{singlet}} = \sigma_0 \zeta(3) \left[\ln \frac{\omega}{m_e} - 1 - C(\nu) \right], \quad (2.20)$$

$$\begin{aligned} C(\nu) &= \frac{1}{2} \int_0^\infty \left\{ 1 - \left[F(i\nu, -i\nu; 1; z) \frac{\pi\nu}{\sinh \pi\nu} \right]^2 \right\} \frac{d\tau}{\tau(1+\tau)^2} \\ &= \frac{1}{4} \int_0^1 \left\{ 1 - \left[F(i\nu, -i\nu; 1; z) \frac{\pi\nu}{\sinh \pi\nu} \right]^2 \right\} \frac{(1+z)dz}{(1-z)\sqrt{z}}. \end{aligned} \quad (2.21)$$

The function $C(\nu)$ is presented in Fig. 4. At small ν it is approximated by

$$C(\nu) = \left[\frac{7}{2} \zeta(3) - 4 + 4 \ln 2 \right] \nu^2 \approx 2.9798 \nu^2. \quad (2.22)$$

Note that the large logarithmic term $\ln(\omega/m_e)$ in the cross section (2.20) arises just from the region of small angles (2.19). Therefore, this region determines the characteristic polar angle of para-Ps production $\theta_{\text{char}}^{1S_0}$.

Up to now we have considered the photoproduction of positronium on nuclei. Let us briefly discuss the photoproduction on atoms where a possible atomic screening has to be taken into account. This can be done by inserting a factor $1 - F(t)$ in the amplitude (2.12) [and $(1 - F(t))^2$ in the cross sections (2.16) or (2.17)], where $F(t)$ is the atomic form factor and t is given in Eq. (2.2). As a result, we obtain the total cross section for photoproduction of para-Ps on atoms:

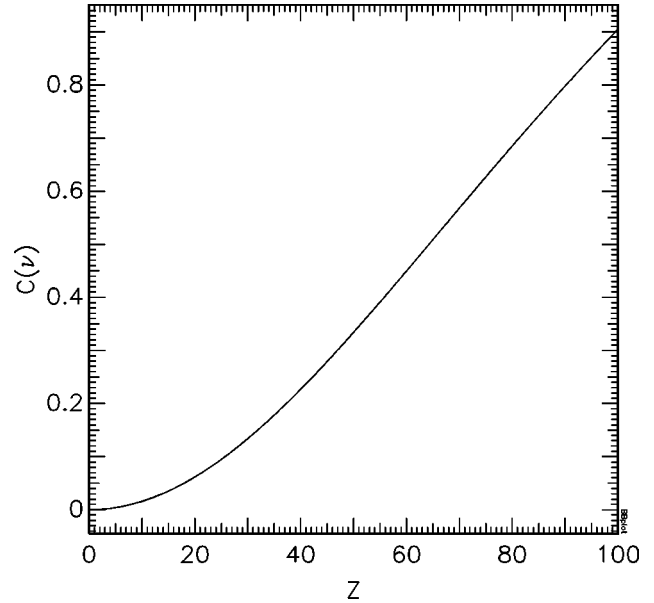


FIG. 4. Function $C(\nu)$ [Eq. (2.21)] vs the nucleus charge number Z .

$$\sigma_{\text{singlet}} = \sigma_0 \zeta(3) [J - C(\nu)], \quad J = \frac{1}{2} \int_0^\infty \frac{\tau [1 - F(t)]^2}{(\tau + \epsilon^2)^2 (1 + \tau)^2} d\tau. \quad (2.23)$$

If we use a simplified Thomas-Fermi-Molière form factor

$$F(t) = \frac{1}{1 - (t/\Lambda^2)}, \quad \Lambda = \frac{Z^{1/3}}{111} m_e, \quad (2.24)$$

we obtain to the accuracy of Eq. (2.1)

$$J = -\frac{1}{2} \ln \left[\left(\frac{m_e}{\omega} \right)^2 + \left(\frac{Z^{1/3}}{222} \right)^2 \right] - 1. \quad (2.25)$$

At not very high energies

$$2m_e \ll \omega \ll \frac{2m_e^2}{\Lambda} = \frac{222}{Z^{1/3}} m_e \quad (2.26)$$

the screening effects are negligible in J and the previous result for the nucleus target (2.20) remains valid. For high enough energies

$$\omega \gg \frac{222}{Z^{1/3}} m_e, \quad (2.27)$$

there is complete screening and the total cross section takes the form

$$\sigma_{\text{singlet}} = \sigma_0 \zeta(3) \left[\ln \frac{222}{Z^{1/3}} - 1 - C(\nu) \right], \quad (2.28)$$

which coincides with the result obtained in [6].

C. Photoproduction of ortho-Ps

The differential cross section of ortho-Ps production on nuclei can be obtained using the amplitude (2.14). For polarized photons it is given by

$$d\sigma_{\text{triplet}} = 4\nu^2 \frac{\sigma_0}{n^3} |\mathbf{e}_\gamma \cdot \mathbf{e}^*|^2 \Phi_i^2 d\tau. \quad (2.29)$$

For unpolarized photons we have

$$d\sigma_{\text{triplet}} = 4\nu^2 \frac{\sigma_0}{n^3} \Phi_i^2 d\tau. \quad (2.30)$$

The dependence of this cross section on τ [and therefore on the polar angle of positronium θ ; see Eq. (2.18)] is given by the function Φ_i^2 ; it is presented in Fig. 5. $d\sigma_{\text{triplet}}/d\tau$ vanishes for all values of ν as $(1-\tau)^2$ at $\tau \rightarrow 1$ [see Eq. (2.8)].

Comparing Eqs. (2.17) and (2.30), we conclude that the angular distributions of ortho-Ps production is considerably wider than that of para-Ps production. Indeed, the typical value of τ for ortho-Ps production is of the order of 0.1, which corresponds to a characteristic emission angle

$$\theta_{\text{char}}^{3S_1} \sim \frac{m_e}{\omega}, \quad (2.31)$$

while for para-Ps production on nuclei the region of very small angles (2.19) gives the main contribution to the cross section.

The total cross section, obtained from Eq. (2.30), is independent of the energy of the initial photon:

$$\sigma_{\text{triplet}} = 4(Z\alpha)^2 \sigma_0 \zeta(3) B(\nu). \quad (2.32)$$

Here the function $B(\nu)$ is

$$B(\nu) = \int_0^\infty \Phi_i^2(\tau, \nu) d\tau = \left(\frac{\pi\nu}{\sinh \pi\nu} \right)^2 \frac{1}{8} \int_0^1 \sqrt{z}(1+z) \times [F(1+i\nu, 1-i\nu; 2; z)]^2 dz. \quad (2.33)$$

Its dependence on Z is shown in Fig. 6. At small $\nu \ll 1$ this function behaves as [6]

$$B(\nu) = 2 - 2 \ln 2 - \left[8(2 - \ln 2)^2 - \frac{2}{3} \pi^2 - 5 \zeta(3) \right] \nu^2 \approx 0.6137 - 1.0729 \nu^2. \quad (2.34)$$

The obtained results for the photoproduction of ortho-Ps on nuclei are also valid for the production on atoms. Indeed, the typical value of $\tau^{3S_1} \sim 0.1$ for photoproduction on nuclei is much larger than the characteristic value

$$\tau_{\text{screen}} \sim \left(\frac{\Lambda}{2m_e} \right)^2 = \left(\frac{Z^{1/3}}{222} \right)^2$$

for which we should take into account the atomic form factor [see Eq. (2.24)].

Now we compare the photoproduction of ortho- and para-Ps on atoms. For energies $\omega \gg 222m_e/Z^{1/3}$ the ratio

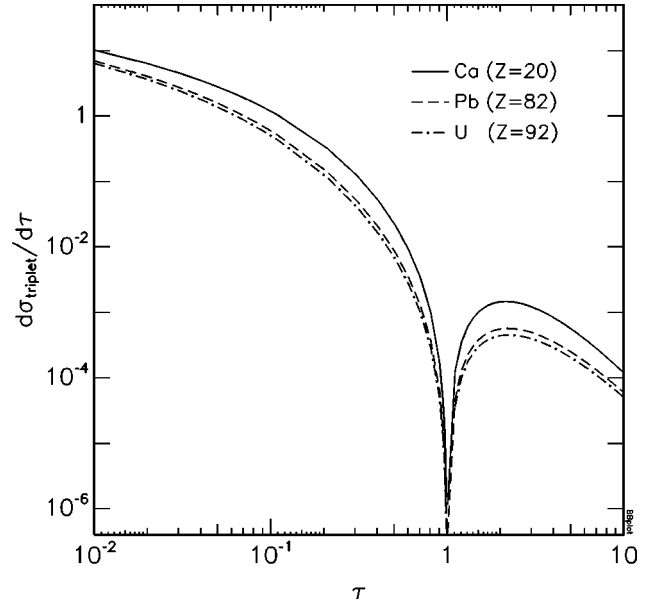


FIG. 5. Differential cross section $d\sigma_{\text{triplet}}/d\tau$ in units $4\nu^2\sigma_0/n^3$.

$$\frac{\sigma_{\text{triplet}}}{\sigma_{\text{singlet}}} = \frac{4\nu^2 B(\nu)}{\ln(222/Z^{1/3}) - 1 - C(\nu)} \quad (2.35)$$

is presented as a function of the nucleus charge number Z in Fig. 7. Some particularly interesting values are 28.5%, 23.5% and 1.51% for U, Pb, and Ca, respectively.

III. ELECTROPRODUCTION OF POSITRONIUM

A. General expressions for the reaction $eA \rightarrow \text{Ps} + eA$

It is well known that the cross section for the electroproduction of Fig. 2 can be exactly written in terms of two structure functions or two cross sections $\sigma_T(\omega, Q^2)$ and $\sigma_S(\omega, Q^2)$ for the processes $\gamma_T^* A \rightarrow \text{Ps} + A$ and $\gamma_S^* A \rightarrow \text{Ps} + A$:

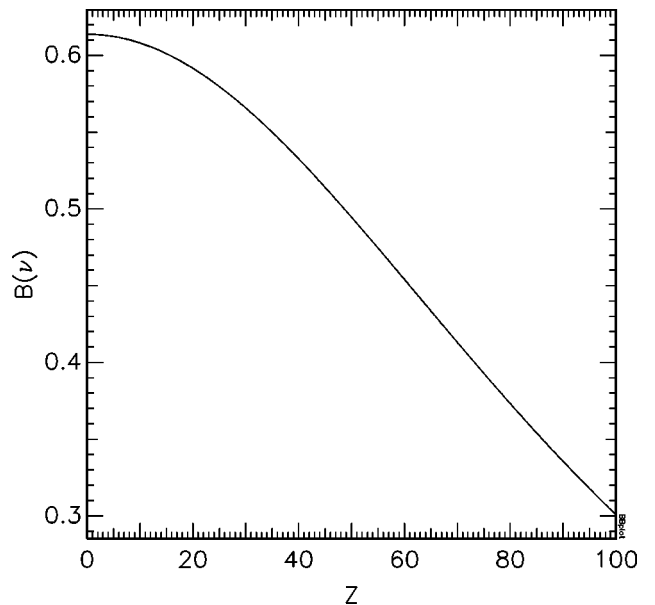


FIG. 6. Function $B(\nu)$ [Eq. (2.33)] vs Z .

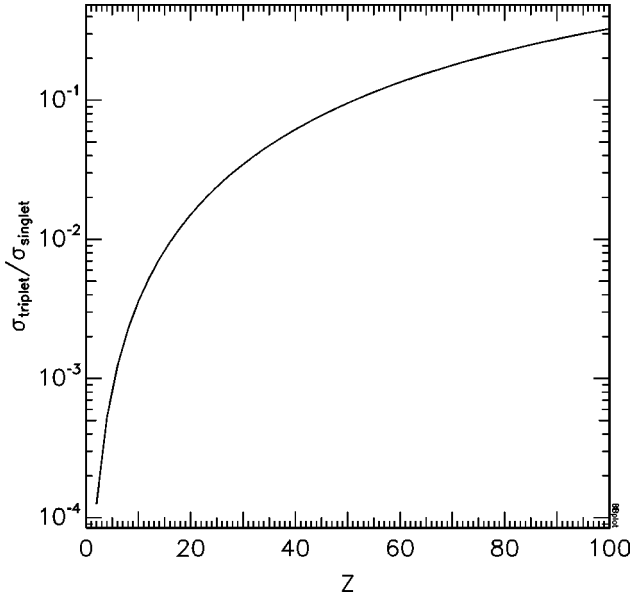


FIG. 7. Ratio $\sigma_{\text{triplet}}/\sigma_{\text{singlet}}$ of photoproduction on atoms at larger energies as a function of Z .

$$d\sigma(eA \rightarrow \text{Ps} + eA) = \sigma_T(\omega, Q^2) dn_T(\omega, Q^2) + \sigma_S(\omega, Q^2) dn_S(\omega, Q^2). \quad (3.1)$$

Here the coefficients dn_T and dn_S can be called the number of transverse and scalar virtual photons, respectively. Using the amplitudes (2.12)–(2.15) for the corresponding processes the cross sections σ_T and σ_S are calculable for virtual photon energies squared

$$\omega^2 \gg (2m_e)^2, Q^2, \quad (3.2)$$

to the accuracy of Eq. (2.1). In the same region and with the accuracy $\sim (2m_e/\omega)^2, Q^2/\omega^2$ the quantities dn_T and dn_S are (see, for example, Sec. VI in Ref. [13])

$$dn_T = \frac{\alpha}{\pi} N \left(\frac{\omega}{E_e}, \frac{Q^2}{4m_e^2} \right) \frac{d\omega}{\omega} \frac{dQ^2}{Q^2}, \quad (3.3)$$

$$N(x, y) = 1 - x + \frac{1}{2}x^2 - \frac{x^2}{4y},$$

$$dn_S = \frac{\alpha}{\pi} \left(1 - \frac{\omega}{E_e} \right) \frac{d\omega}{\omega} \frac{dQ^2}{Q^2}. \quad (3.4)$$

The variable y is defined in Eq. (1.4). Since the energy E of the positronium almost coincides with that of the virtual photon, the energy fraction transferred from the electron to Ps is

$$x = \frac{E}{E_e} = \frac{\omega}{E_e}. \quad (3.5)$$

B. Electroproduction of para-Ps

The cross sections σ_T and σ_S for para-Ps production are obtained using Eqs. (2.12) and (2.13) and repeating the calculations of Sec. II B with $Q^2 > 0$. This leads to

$$d\sigma_T = \frac{\sigma_0}{2n^3(1+y)^2} \Phi_s^2 d\tau, \quad d\sigma_S = 0 \quad (3.6)$$

[with τ defined in Eq. (2.2)] and to the integrated cross sections

$$\sigma_T = \frac{\sigma_0}{(1+y)^2} \zeta(3) [L - 1 - C(\nu)], \quad \sigma_S = 0. \quad (3.7)$$

Here, for the electroproduction on nuclei [compare Eqs. (2.17) and (2.20)]

$$L = \ln \frac{\omega}{m_e} - \frac{1}{2} \ln(1+y) \quad (3.8)$$

and on atoms [compare Eqs. (2.23) and (2.25)]

$$L = -\frac{1}{2} \ln \left[\left(\frac{m_e}{\omega} \right)^2 (1+y) + \left(\frac{\Lambda}{2m_e} \right)^2 \frac{1}{(1+y)} \right]. \quad (3.9)$$

Using Eqs. (3.1)–(3.9) we are able to obtain the energy-angular and energy distributions of relativistic Ps. In particular, the spectrum of para-Ps is

$$d\sigma(eA \rightarrow {}^1S_0 + eA) = \frac{\alpha}{\pi} \sigma_0 \zeta(3) F_s(x) \frac{dx}{x}, \quad (3.10)$$

$$F_s(x) = \int_{y_m}^{\infty} \frac{[L - 1 - C(\nu)]}{(1+y)^2} N(x, y) \frac{dy}{y}, \quad y_m = \frac{x^2}{4(1-x)}.$$

Since the cross section rapidly decreases above $y \approx 1$, the upper integration limit can be extended to infinity.

For the electroproduction on nuclei the y integration is easily performed and we obtain

$$F_s(x) = f_1(x) \left[\ln \frac{x E_e}{m_e} - 1 - C(\nu) \right] - f_2(x). \quad (3.11)$$

The functions $f_1(x)$ and $f_2(x)$ are

$$f_1(x) = 2(1-x+x^2) \ln \frac{2-x}{x} - \frac{4(1-x)}{(2-x)^2} (2-2x+x^2), \quad (3.12)$$

$$f_2(x) = (1-x+x^2) \left[\frac{\pi^2}{12} - \frac{2(1-x)}{(2-x)^2} - \frac{1}{2} \text{Li}_2 \left(\frac{x^2}{(2-x)^2} \right) \right] + \frac{x^2}{4} \left(\frac{2(1-x)}{(2-x)^2} + \ln \frac{x}{2-x} \right) - \frac{2(1-x)}{(2-x)^2} \times (2-2x+x^2) \ln \frac{(2-x)^2}{4(1-x)},$$

with the dilogarithm function

$$\text{Li}_2(z) = \int_z^{0 \ln(1-t)} \frac{dt}{t}.$$

Note that $f_2(x) < f_2(0) = (\pi^2 - 6)/12 = 0.3225$.

The same result (3.11) is valid for electroproduction on atoms at $2m_e \ll xE_e \ll 222m_e/Z^{1/3}$ (no screening). For the case of complete screening ($xE_e \gg 222m_e/Z^{1/3}$) we have

$$F_s(x) = f_1(x) \left[\ln \frac{222}{Z^{1/3}} - 1 - C(\nu) \right] + f_2(x). \quad (3.13)$$

In the important case of small x (i.e., at $2m_e/E_e \ll x \ll 1$) the spectrum is simplified:

$$F_s(x) = \left(2 \ln \frac{2}{x} - 2 \right) \left[\ln \frac{x E_e}{m_e} - 1 - C(\nu) \right] - \frac{\pi^2 - 6}{12} \quad (3.14)$$

for no screening and

$$F_s(x) = \left(2 \ln \frac{2}{x} - 2 \right) \left[\ln \frac{222}{Z^{1/3}} - 1 - C(\nu) \right] + \frac{\pi^2 - 6}{12} \quad (3.15)$$

for complete screening. The accuracy of the obtained spectrum is determined by omitting terms of the order of

$$\frac{2m_e}{xE_e}. \quad (3.16)$$

It is interesting to compare our spectra (3.10)–(3.15) with that given in [8]

$$F_s^{\text{HO}}(x) = \left(2 \ln \frac{1}{x} - 1 \right) \left\{ -\frac{1}{2} \ln \left[\left(\frac{m_e}{xE_e} \right)^2 + \left(\frac{Z^{1/3}}{222} \right)^2 \right] - 1 \right\}. \quad (3.17)$$

The spectrum $F_s^{\text{HO}}(x)$ was obtained by neglecting the exact dependence of σ_T on Q^2 and high-order ν corrections. As a consequence, the accuracy of Eq. (3.17) is only logarithmic [in expressions (3.14), (3.15), and (3.17) the leading logarithmic terms coincide, whereas the next to leading logarithmic terms are different even at $\nu \ll 1$]. Therefore, this approximation is not well suited for heavy atoms. For example, in the case of complete screening the spectrum $F_s^{\text{HO}}(x)$ exceeds our spectrum $F_s(x)$ up to approximately 40% for U and 30% for Pb in the x region below 0.4.

C. Electroproduction of ortho-Ps

The ortho-Ps production in collisions of electrons with atoms due to the bremsstrahlung mechanism of Fig. 3 was calculated in [7,8]. The principal features of this mechanism are the following. The spectrum of ortho-Ps has a peak in the region of high-energy fractions (at $x \approx 1$) and the characteristic emission angle of Ps is small

$$\theta_{\text{char}}^{\text{br}} \sim \frac{m_e}{E_e}. \quad (3.18)$$

The total cross section is equal to [8]

$$\sigma_{\text{br}} = \frac{\alpha}{\pi} \sigma_0 \zeta(3) I_{\text{br}}, \quad (3.19)$$

where

$$I_{\text{br}} = 0.303 \ln \frac{E_e}{m_e} - 0.542 \quad (3.20)$$

for no screening ($E_e \ll 444m_e/Z^{1/3}$) and

$$I_{\text{br}} = 0.303 \ln \frac{111}{Z^{1/3}} + 0.362 \quad (3.21)$$

for complete screening ($E_e \gg 444m_e/Z^{1/3}$).

In this section we argue that in many respects these results are incomplete or even misleading because in [7,8] the important multiphoton (MP) production of ortho-Ps due to diagrams of Fig. 2 with even numbers $j=2,4,6,\dots$ of exchanged photons was not considered. Moreover, we find out that MP production is dominant for electron scattering on heavy atoms.

To study the MP production of ortho-Ps, we have to calculate the cross sections σ_T and σ_S for ortho-Ps production [see Eq. (3.1)]. This is achieved using the corresponding amplitudes (2.14) and (2.15) and repeating the calculations of Sec. II C with $Q^2 > 0$. For the cross sections we obtain [compare Eqs. (2.30) and (2.32)]

$$d\sigma_T = 4\nu^2 \frac{\sigma_0}{n^3(1+y)^3} \Phi_T^2 d\tau, \quad d\sigma_S = y d\sigma_T, \quad (3.22)$$

$$\sigma_T = 4\nu^2 \frac{\sigma_0}{(1+y)^3} \zeta(3) B(\nu), \quad \sigma_S = y \sigma_T. \quad (3.23)$$

Using these formulas and Eq. (3.1) we can again obtain the energy-angular and energy distributions for the triplet state of relativistic positronium. In particular, now the spectrum of ortho-Ps is

$$d\sigma_{\text{MP}} = \frac{4\alpha}{\pi} (Z\alpha)^2 \sigma_0 \zeta(3) B(\nu) F_t(x) \frac{dx}{x}, \quad (3.24)$$

$$F_t(x) = 2 \left(1 - x + \frac{5}{4}x^2 \right) \ln \frac{2-x}{x} - \frac{(1-x)}{(2-x)^4} [32(1-x)^2 + 34(1-x)x^2 + 5x^4]. \quad (3.25)$$

The spectrum [function $F_t(x)/x$] is shown in Fig. 8. The result (3.24) and (3.25) is valid for collisions of electrons with both nuclei and atoms. The behavior of the function $F_t(x)$ at small and large x is

$$F_t(x) = 2 \ln \frac{2}{x} - 2 \quad \text{at } \ll 1, \quad (3.26)$$

$$F_t(x) = \frac{56}{3} (1-x)^3 \quad \text{at } 1-x \ll 1.$$

Contrary to the bremsstrahlung spectrum (see Fig. 3 in [8]), the spectrum (3.24) is peaked at small energies of Ps. Therefore, the interference of bremsstrahlung and MP production should be very small.

Taking into account Eqs. (2.31) and (3.5), we conclude that the characteristic angle for MP production of ortho-Ps is

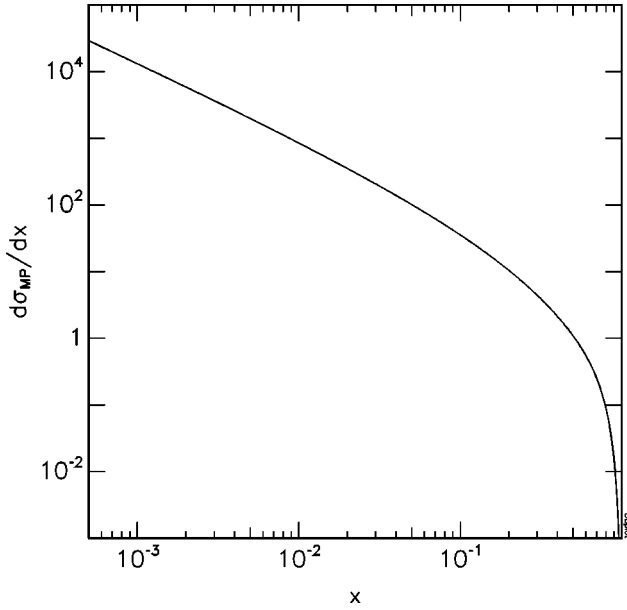


FIG. 8. Ortho-Ps spectrum in electroproduction in units $(4\alpha/\pi)\sigma_0\zeta(3)\nu^2B(\nu)$ due to the multiphoton mechanism of Fig. 2.

$$\theta_{\text{char}}^{\text{MP}} \sim \frac{m_e}{xE_e}, \quad (3.27)$$

which is much larger than Eq. (3.18). In other words, the angular distribution of MP production is considerably wider than that of the bremsstrahlung reaction.

In this section the spectra for relativistic positronium in electroproduction have been calculated with the high accuracy of Eq. (3.16). This accuracy cannot be achieved for the total cross sections in the scheme used here by the following reasons. The spectrum has to be integrated over the whole kinematic region in x including that of the threshold $x \sim 2m_e/E_e$. However, near the threshold the accuracy of our calculated spectra becomes only logarithmic. Furthermore, in this region Ps is not a relativistic particle and therefore its detection is difficult. However, if we are interested in finding the total cross section with logarithmic accuracy, we can integrate the spectra in the whole region

$$x_m = \frac{2m_e}{E_e} \leq x \leq 1. \quad (3.28)$$

Having in mind this restriction, we find for the total cross section of MP production

$$\sigma_{\text{MP}} \approx \frac{4\alpha}{\pi} (Z\alpha)^2 \sigma_0 \zeta(3) B(\nu) I_{\text{MP}},$$

$$I_{\text{MP}} = \int_{x_m}^1 F_t(x) \frac{dx}{x} \approx \left(\ln \frac{E_e}{m_e} \right)^2 - 2 \ln \frac{E_e}{m_e} - c, \quad (3.29)$$

$$c = \frac{\pi^2}{6} - \frac{5}{4} = 0.3949.$$

Note that this multiphoton cross section increases with the energy of the projectile electron as $[\ln(E_e/m_e)]^2$, while the

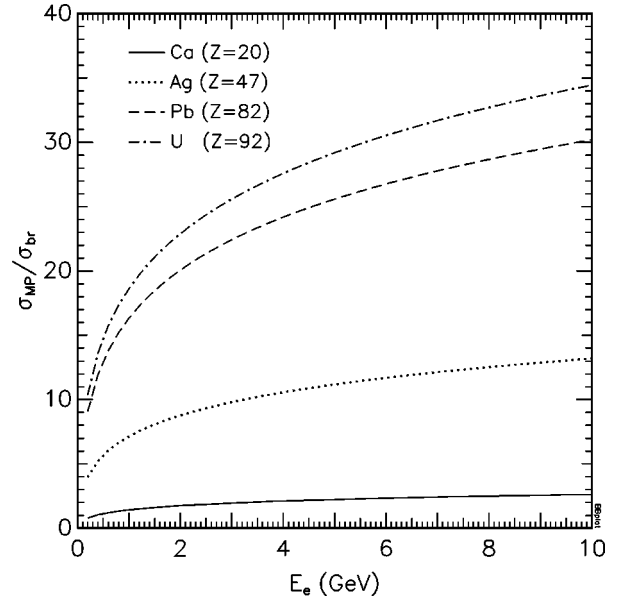


FIG. 9. Ratio $\sigma_{\text{MP}}/\sigma_{\text{br}}$ of the multiphoton (Fig. 2) to bremsstrahlung cross section (Fig. 3) as a function of the electron beam energy E_e .

cross section for the bremsstrahlung production on atoms is constant at high energies [see Eq. (3.21)]. The dependence of the cross section ratio

$$\frac{\sigma_{\text{MP}}}{\sigma_{\text{br}}} = 4\nu^2 B(\nu) \frac{I_{\text{MP}}}{I_{\text{br}}}, \quad (3.30)$$

on the initial electron energy E_e is presented in Fig. 9 for different values of Z . From that figure it can be seen that the MP production is the dominant production mechanism of orthopositronium for atoms with nucleus charge number $Z > 20$.

IV. SUMMARY

In this paper we have presented an almost complete description of the production of relativistic positronium in high-energy photon and electron collisions with nuclei and atoms. The high accuracy of our results is restricted by neglecting terms of the order of the inverse Ps Lorentz factor $2m_e/E$.

The matrix elements of the virtual photon nucleus scattering to produce both para- and ortho-Ps are given in Eqs. (2.12)–(2.15) including polarizations of the initial photon and the positronium and summed high-order $Z\alpha$ corrections. The singlet positronium state can be produced only by transversely polarized initial photons. The transition amplitude depends on the azimuthal angle of 1S_0 . The amplitude for scalar virtual photons to para-Ps is zero. The transitions from the initial virtual transverse and scalar photon to the triplet state are accompanied with helicity conservation $\lambda_\gamma = \lambda$; the amplitudes do not depend on the azimuthal angle of ortho-Ps.

These results are used to discuss both photo- and electroproduction of Ps. Various distributions and total cross sections are calculated and compared to previous results. The screening effects are estimated analytically using a Thomas-Fermi-Molière atomic form factor.

For the photoproduction of relativistic positronium we have found that the polar angular distribution of ortho-Ps is considerably wider than that of para-Ps. The high-order $Z\alpha$ effects decrease the ortho-Ps photoproduction cross section by 3.61% for Ca, 40.5% for Pb, and 46.5% for U nuclei. The ratio of the total cross sections for the triplet to singlet state at higher energies $\omega \gg 222m_e/Z^{1/3}$ in the $\gamma A \rightarrow {}^3S_1 + A$ process increases with the nucleus charge number from 1.51% for Ca, 23.5% for Pb to 28.5% for U targets.

In the para-Ps electroproduction the virtuality of the photons arising from the electron projectile and the effects of heavy nuclei are quite important. As an example, the spectrum [8] estimated in an equivalent photon approximation and with neglected high-order $Z\alpha$ effects exceeds the correctly calculated result up to 30% for Pb and 40% for U in a wide range of the energy fraction transferred from the electron to Ps.

Finally, we have proposed a multiphoton mechanism for the production of ortho-Ps in the reaction $eA \rightarrow {}^3S_1 + eA$, which has to be taken into account in addition to the bremsstrahlung production discussed by Holvik and Olsen. Due to a completely different angular and energy distribution of MP, its interference with the bremsstrahlung reaction is expected to be small. This mechanism is dominant for electron

scattering on heavy atoms. Therefore, our results complete and correct those earlier studies.

Finally, we would like to note that our results cannot be straightforwardly transformed to the production of the $\mu^+\mu^-$ elementary atom called dimuonium (DM). For the photo- and electroproduction of DM an important phenomenon takes place, namely, the restriction of the transverse momenta $k_{1\perp}, \dots, k_{j\perp}$ for the exchanged photons in Figs. 1 and 2. This restriction arises due to the nucleus form factor at the level $\leq 1/r_A \ll m_\mu$, where r_A is the electromagnetic radius of the nucleus. As a result, the effective parameter of the perturbation theory becomes small $\sim v^2/(r_A m_\mu)^2 \lesssim 0.03$, contrary to the Ps case. A detailed study of DM production will be presented in [14].

ACKNOWLEDGMENTS

We are grateful to R. Faustov, I. Ginzburg, I. Khriplovich, I. Meshkov, and L. Nemenov for useful discussions and to A. Arbuzov, O. Krehl, and B. Shaikhatdenov for help. The work of S.R.G. and E.A.K. was supported by INTAS under Grant No. 93-239 ext. The work of V.G.S was supported by Volkswagen Stiftung (Grant No. 1/72 302) and by the Russian Foundation for Basic Research (Grant No. 96-02-19114).

-
- [1] I. N. Meshkov, *Elem. Particles and Nuclei* **28**, 495 (1997).
 - [2] I. B. Khriplovich, A. I. Milstein, Novosibirsk Budker Institute of Nuclear Physics Report No. INP 96-49, 1996 (unpublished).
 - [3] L. L. Nemenov, *Yad. Fiz.* **51**, 444 (1990), [*Sov. J. Nucl. Phys.* **51**, 284 (1990)]; V. L. Lyuboshitz and M. I. Podgoretsky, *Zh. Eksp. Teor. Fiz.* **81**, 1556 (1981).
 - [4] G. V. Meledin, V. G. Serbo, and A. K. Slivkov, *Pis'ma Zh. Eksp. Teor. Fiz.* **13**, 98 (1971) [*JETP Lett.* **13**, 68 (1971)].
 - [5] H. A. Olsen, *Phys. Rev. D* **33**, 2033 (1986).
 - [6] A. V. Tarasov and I. V. Christova, Joint Institute for Nuclear Research Report No. P2-91-4, (1991) (unpublished).
 - [7] A. A. Akhundov, D. Yu. Bardin, and L. L. Nemenov, *Yad. Fiz.* **27**, 1542 (1978).
 - [8] E. Holvik and H. A. Olsen, *Phys. Rev. D* **35**, 2124 (1987).
 - [9] D. Ivanov and K. Melnikov, *Phys. Rev. D* **57**, 4025 (1998).
 - [10] H. A. Bethe and L. C. Maximon, *Phys. Rev.* **93**, 788 (1954); H. A. Olsen and L. C. Maximon, *ibid.* **114**, 887 (1959).
 - [11] V. B. Berestetskii, E. M. Lifshitz, and L. B. Pitaevskii, *Quantum Electrodynamics* (Nauka, Moscow, 1989).
 - [12] V. A. Novikov *et al.*, *Phys. Rep.*, *Phys. Lett.* **41C**, 1 (1978).
 - [13] V. M. Budnev, I. F. Ginzburg, G. V. Meledin, and V. G. Serbo, *Phys. Rep.*, *Phys. Lett.* **15C**, 181 (1975).
 - [14] I. F. Ginzburg, V. D. Jentschura, S. G. Karshenboim, F. Krauss, V. G. Serbo, and G. Soff, hep-ph/9805375, *Phys. Rev. C* (to be published).